Microfluidic fabrication of polymeric core-shell microspheres for controlled release applications[a)]

Tiantian Kong,[1,2,b)] Jun Wu,[3] Kelvin Wai Kwok Yeung,[3]
Michael Kai Tsun To,[3,c)] Ho Cheung Shum (岑浩璋),[1,4,c)] and Liqiu Wang[1,2,c)]
[1]*Department of Mechanical Engineering, The University of Hong Kong, Pokfulam Road, Hong Kong*
[2]*HKU-Zhejiang Institute of Research and Innovation (HKU-ZIRI), 311100 Linan, Zhejiang, China*
[3]*Department of Orthopaedics and Traumatology, Li Ka Shing Faculty of Medicine, HKU, HK, China*
[4]*HKU-Shenzhen Institute of Research and Innovation (HKU-SIRI), 518000 Shenzhen, Guangdong, China*

(Received 22 April 2013; accepted 7 August 2013; published online 26 August 2013)

We report a facile and robust microfluidic method to fabricate polymeric core-shell microspheres as delivery vehicles for biomedical applications. The characteristics of core-shell microspheres can be precisely and easily tuned by manipulating the microfluidic double emulsion templates. The addition of a shell can significantly improve the versatility as well as functionality of these microspheres as delivery vehicles. We demonstrate that the nature of the shell material plays an important role in the properties of the core-shell delivery vehicles. The release kinetics is significantly influenced by the material of the shell and other characteristics such as the thickness. For example, by adding a poly(lactic-co-glycolic acid) (PLGA) shell to an alginate core, the encapsulation efficiency is enhanced and undesired leakage of hydrophilic actives is prevented. By contrast, adding an alginate shell to PLGA core can lead to a reduction of the initial release rate, thus extending the release period of hydrophobic actives. Microfluidic fabrication enables the generation of precisely controlled core-shell microspheres with a narrow size distribution, which enables the investigation of the relationship between the release kinetics of these microspheres and their characteristics. The approach of using core-shell particles as delivery vehicles creates new opportunities to customize the release kinetics of active ingredients. [http://dx.doi.org/10.1063/1.4819274]

INTRODUCTION

Polymer-based systems have been extensively studied as delivery vehicles of drugs, proteins, peptides, and small interfering ribonucleic acid (siRNA).[1–4] Polymer-based microspheres are convenient to fabricate, generally biocompatible, with tunable physical and chemical properties. These attributes make them attractive for encapsulation and controlled release applications.[3–6] Active ingredients can be trapped in the polymer matrices and released subsequently by diffusion or degradation of polymer matrices. However, it remains a challenge to tailor the release profiles from these polymeric microspheres to the need of applications. For instance, undesired initial burst release of active ingredients from polymer microspheres remains difficult to avoid.[7–9] This challenges the ability to release ingredients in a sustained manner.[7–10] Core-shell polymer-based microspheres, with the additional shell whose properties can be tuned, offers more control over

[a)]Paper submitted as part of the 3rd European Conference on Microfluidics (Guest Editors: J. Brandner, S. Colin, G. L. Morini). The Conference was held in Heidelberg, Germany, December 3–5, 2012.
[b)]Electronic mail: emmakong@hku.hk
[c)]Authors to whom correspondence should be addressed. Electronic addresses: miketto@hku.hk, ashum@hku.hk, and lqwang@hku.hk.

the release kinetics of the encapsulated active ingredients in the core. Active ingredients have to diffuse through both the core and shell before they are released. By choosing proper shell materials, the initial release rate can be reduced significantly and the overall release period can be prolonged. Release kinetics can be further adjusted by varying other characteristics of the shell, such as its thickness. Besides, core-shell microspheres have several additional advantages. Fragile therapeutic agents protected in the cores can be completely isolated by the shell from the surrounding environment. Functional groups and reagents can be attached to the surface of the shell to achieve targeted delivery. Active ingredients with different functions and properties can be encapsulated separately in the core and the shell to realize co-delivery. Therefore, introduction of an additional shell layer on polymeric microspheres can significantly improve their versatility as well as functionality as delivery vehicles.

Although polymer-based core-shell microspheres show great promise in biomedical applications, the conventional fabrication method has limited their utilization. Conventional techniques for generating double emulsion employs high shear, reducing the encapsulation efficiency.[11,12] The resultant core-shell microspheres are polydisperse in size with little control over their characteristics; moreover, the reproducibility is also poor. Therefore, a facile method for fabricating monodisperse core-shell microspheres with precise control over the structure is desired.

Recent advances in microfluidics enable fabrication of monodisperse oil-in-water-in-oil (O/W/O) or water-in-oil-in-water (W/O/W) double emulsion droplets in a highly controlled fashion.[13–17] These droplets are perfect templates for core-shell microspheres.[16,17] Two different polymers can be dissolved in two separate solvents, which will become the inner and middle phases after microfluidic double emulsification. The resultant double emulsions can be solidified to form core-shell microspheres. Active ingredients of different solubility can be encapsulated separately in the core and the shell. One important advantage of microfluidics is the ability to generate droplets one-by-one;[18] this offers intricate control over the structure of the final microspheres. The characteristics, such as core size and shell thickness, can be easily and precisely manipulated. This allows the investigation of the relationship between the structure and the release kinetics of the delivery vehicles. Another important advantage of microfluidics is the narrow size distribution; this enables investigation of the relationship between size and release kinetics.

In this paper, we choose two common biocompatible polymers, alginate extracted from algae and poly(lactic-co-glycolic acid) (PLGA), a Food and Drug Administration (FDA)-approved material with tunable degradation rate, as model materials to form core-shell spheres. Alginate microgel spheres have been extensively employed to encapsulate cells, biomolecules and hydrophilic drugs.[19–22] PLGA is well-developed for controlled release of hydrophobic drugs.[6,7,11] Despite the pervasiveness of these two polymers, studies using alginate/PLGA or PLGA/alginate core-shell microspheres as delivery vehicles for controlled release applications remain limited. We fabricate alginate/PLGA and PLGA/alginate core-shell microspheres from W/O/W and O/W/O double emulsion droplets, respectively. We show that the structure of our microspheres can be tuned easily either by changing the flow rates, device geometry, or osmotic pressure. We show that hydrophilic and hydrophobic active ingredients can be encapsulated in the cores and shells, respectively. We further demonstrate that the initial burst release is reduced and the overall release period from our core-shell microspheres is prolonged. Therefore, these core-shell microspheres are suitable for applications where sustained release profiles are required. Our core-shell microspheres provide a microscale platform for co-delivery and controlled release of therapeutic agents of different solubility.

EXPERIMENTS

Materials

Poly(vinyl alcohol) (PVA, 87%–89%, hydrolyzed, average Mw = 13 000–23 000), poly(D,L-lactide-co-glycolide) (PLGA, ester terminated, L/G = 50:50, Mw 7000–17 000), rifampicin (≥97%, powder), anhydrous calcium chloride, nonionic surfactant sorbitane monooleate (Span 80) and Oil Red O are purchased from Sigma-Aldrich. Alginate in the form of alginic

acid sodium salt was purchased from Fluka. Surfactant Dow Corning 749 fluid is purchased from Dow Corning Corporation. Dichloromethane (DCM) is purchased from Lab-scan Analytical Science. Toluene is purchased from BDH Prolabo Chemicals.

Generation of double emulsions

We use a capillary microfluidic device to generate monodisperse W/O/W and O/W/O double emulsions, respectively.[13–18] In a typical capillary microfluidic double-emulsion device, two cylindrical capillaries (World Precision Instrument, Inc.), which have an inner diameter and an outer diameter of 0.58 mm and 1 mm, respectively, are tapered using a micropipette puller (P-97, Sutter Instrument, Inc.). The tips of the capillaries are polished to desired diameters using a sand paper. Typical tip diameters of the injection and collection capillaries are 25 μm and 100 μm, respectively. Then the polished round capillaries are coaxially aligned inside a square capillary (AIT glass). By combining the co-flow and flow-focusing geometries, the device can be used for generating monodisperse double emulsions, as shown by the schematic in Figure 1(A). By hydrophobizing different parts of the capillaries using n-octadecyltrimethoxy silane (Aldrich), the resultant device was used to generate oil-in-water-in-oil (O/W/O) or water-in-oil-in-water (W/O/W) double emulsions, respectively.

This device geometry works well when the viscosities of the fluid phases are of similar values. Typically, the inner phase is pumped through one tapered round capillary, often known as the injection capillary; the middle phase flows through the region between the injection capillary and the square capillary in the same direction. The inner aqueous droplets form by dripping from the tip of the inner round injection capillary in the co-flow geometry. The outer aqueous phase flows through the region between the other round capillary, often known as the collection capillary, and the square capillary, in the opposite direction. The outer phase hydrodynamically focuses the middle phase containing the innermost droplets; the resultant jet breaks up into monodisperse double-emulsion drops at the orifice of the collection capillary, as shown by the schematic in Figure 1(A).

We use this device geometry to generate W/O/W double emulsion templates to fabricate alginate-PLGA core-shell microspheres. The inner phase of the double emulsion templates consists of deionized (DI) water with 0.5% sodium alginate and 10% (w/v) PVA; DCM with 20% (w/v) PLGA (50:50) is used as the middle oil phase. DCM is a frequently used organic solvent for PLGA and evaporates quickly at room temperature. The outermost aqueous phase consists of DI water with 10% (w/v) PVA and 4% calcium chloride ($CaCl_2$). The viscosities of the inner, middle, and outer phases in our experiments are 1.44 mm^2/s, 1.8 mm^2/s, 3.36 mm^2/s, respectively. Typical flow rates of the three phases we use to generate the W/O/W double emulsions are 200, 800, and 2000 μl/h, respectively.

However, when the viscosity of the middle phase exceeds the viscosity of the outer phase significantly, fluid flow in devices with this geometry becomes ill-controlled. To generate O/W/O double emulsions templates for fabrication of PLGA-alginate core-shell microspheres. We use dichloromethane with 8% (w/v) PLGA as inner phase, 0.5% (w/v) sodium alginate, and 1% (w/v) PVA as middle phase and the outer phase is made up of toluene with 10% (w/v) span 80. The

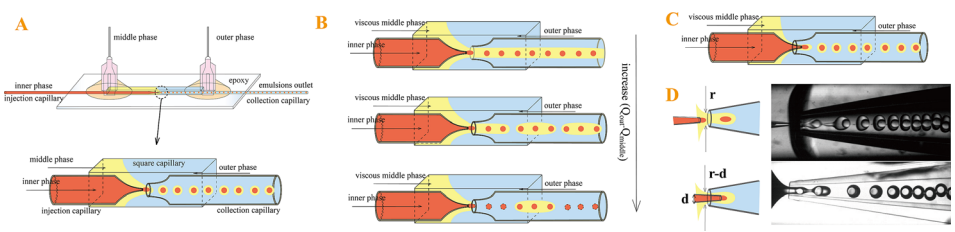

FIG. 1. (A) Schematic of a typical capillary microfluidic device geometry and generation of double emulsion droplets; (B) schematic of ill-controlled fluid flow with increasing difference in the flow rates of the outer and middle phases when the viscosity of middle phase is 27.5 times higher than that of the outer phase; (C) schematic of the modified capillary microfluidic device geometry; and (D) comparison of the typical and modified device geometries.

viscosities of inner, middle, and outer phases are 1.8 mm^2/s, 27.5 mm^2/s, and 1 mm^2/s, respectively. In this case, the middle phase is highly viscous; to break up the middle phase jet, the flow rate difference between the middle and outer phases ($Q_{outer} - Q_{middle}$) must be significantly increased. However, when the difference in flow rates is too large, the middle phase ceases to form a stable jet, as shown in Figure 1(B). A common method to address this problem is to minimize the difference in viscosities by choosing the appropriate compositions in the different phases. However, this significantly limits the choice of the materials.

To solve this problem, we modify the geometry of the device slightly and insert the injection capillary into the collection capillary, as shown in Figure 1(C). With this new geometry, the velocity of the middle phase v increases significantly due to the decrease in the jet radius r, under the same flow rate Q, $v = 4Q/\pi r^2$, as shown by the resultant jets in Figure 1(D). The decrease in the middle jet diameter is due to the insertion of injection capillary. The flow rates of the three phases we use in generating O/W/O double emulsions are 400, 500, and 500 μl/h, respectively.

Characterization of core-shell microspheres

The morphology of the resultant core-shell microspheres is characterized using an optical microscope (Nikon Eclipse 80i) and a scanning electron microscope (Hitachi S3400N VP SEM). To obtain the size distribution of the microspheres, we measure at least 100 microspheres for each diameter by analyzing microscope images using the open-source image analysis software, Image J.

RESULTS AND DISCUSSION

To encapsulate, deliver and release active ingredients in a sustained manner, one of the most frequently employed methods is to trap active ingredients in polymer matrices with tunable degradation rate in the form of microspheres.[1–10] PLGA is a well-developed biocompatible polymer with a tunable degradation rate, and is extensively employed in the controlled release of drugs.[6,7,11]

However, single PLGA microspheres are typically limited by a low loading efficiency for hydrophilic actives due to the hydrophobic nature of PLGA, and it remains difficult to tailor their release kinetics and avoid undesired release patterns.[7–10] These difficulties can be overcome by using composite microspheres with complex structures, such as core-shell composite microspheres. To enhance the encapsulation efficiency for hydrophilic actives, a core of hydrophilic nature can be incorporated inside the PLGA microspheres. To avoid undesired release patterns from PLGA microspheres, a shell made from materials enabling different release mechanisms can be added to modulate release kinetics.

Double emulsion droplets are excellent templates for fabricating core-shell microspheres. W/O/W or O/W/O double emulsion templates can be employed, depending on the solubility of active ingredients to be encapsulated. Monodisperse, size-controlled W/O/W and O/W/O double emulsions are routinely generated using capillary microfluidic techniques. The exquisite control of droplet generation allows manipulation over the characteristics of the final microspheres, such as their size and core-to-shell ratio. To tailor these characteristics, we use a simple theoretical model to predict the size of emulsion droplets under flow-induced dripping regime.[18,23] In the dripping regime, when the capillary number, *Ca*, which is the ratio of shear F_{shear} and interfacial forces F_r, reaches a critical value, typically on the order of 1, droplets detach from the nozzle and flow downstream. The size of the generated emulsion droplet can be predicted by solving Eq. (1),[18,23]

$$F_{shear} = Ca_{critical} F_r. \tag{1}$$

For double emulsions, when the breakup of the middle phase forces the inner phase to break up, we can treat the middle phase containing the innermost phase as a single dispersed

phase detaching from the nozzle. In this case, the shear force and interfacial tension on middle phase fluid, $F_{2,shear}$ and $F_{2,r}$, are represented by Eqs. (2) and (3), respectively,

$$F_{2,shear} = 3\pi\mu_3(d_2 - d_{2thread})(v_3 - v_2), \tag{2}$$

$$F_{2,\gamma} = \pi d_{2thread}\gamma_{2,3}, \tag{3}$$

where μ_3 is the viscosity of the outer phase fluid, d_{cap} is the diameter of the injection capillary, and $d_{2thread}$ is the diameter of the fluid thread formed in the co-flowing middle fluids. The value of $d_{2thread}$ can be approximated by mass balance: $d_{2thread} = D_c\sqrt{(Q_1+Q_2)/(Q_1+Q_2+Q_3)}$, where D_c is the diameter of the collection capillary. Q_1, Q_2, Q_3 are the volumetric flow rates of the inner, middle, outer phase fluids, respectively. $\Upsilon_{2,3}$ define the surface tension between middle and outer fluids. v_2, v_3 represent the average velocities of the middle and the outer phases, respectively, where $v_2 = 4Q_2/\pi(d_2^2 - d_1^2)$, $v_3 = 4Q_3/\pi(D_c^2 - d_2^2)$.

By solving Eqs. (1)–(3), the size of the whole droplet size d_2 can be predicted (Eq. (4)), while the size of inner droplet size, d_1, can be predicted using mass balance, as shown by Eq. (5).[23,24]

$$d_2^4 + \Gamma_{2,3}(Q_3+Q^*)d_2^3 - (\Gamma_{2,3}d_{2thread}(Q_3+Q^*) + D_c^2)d_2^2 - \Gamma_{2,3}Q^*D_c^2d_2 + \Gamma_{2,3}Q^*D_c^2d_{2thread} = 0, \tag{4}$$

$$Q^* = Q_2/[1-(Q_1/(Q_2+Q_1))^{2/3}], \quad \Gamma_{2,3} = 12\mu_3/\pi Ca_{2,3}(d_{2thread}\gamma_{2,3} + d_{cap}\gamma_{1,2})$$
$$d_1 = [Q_1/(Q_1+Q_2)]^{\frac{1}{3}}d_2. \tag{5}$$

However, if the inner phase breaks up first and triggers the middle phase to pinch off, the prediction by Eqs. (4) and (5) is not accurate. This case is common in the modified geometry as shown in Figure 1(C). The velocity of middle phase jet is accelerated under the same flow rate, implying that middle phase exerts a higher shear force on the inner phase. Thus, the inner phase fluid is more likely to pinch off in the modified geometry. Moreover, when the viscosity of middle fluid is high, the middle phase jet will break up considerably more slowly even under a large shear force. This also causes the inner fluid to break up before the middle fluid does.

Therefore, for the cases where the break-up of inner phase triggers the formation of double emulsion droplets, we predict the inner droplet size d_1 and the overall droplet size d_2 based on the critical capillary number and mass balance, respectively,

$$F_{1,shear} = 3\pi\mu_2(d_1 - d_{cap})(v_2 - v_1), \tag{6}$$

$$F_{1,\gamma} = \pi d_{cap}\gamma_{1,2}, \tag{7}$$

where $F_{1,shear}$ and $F_{1,\Upsilon}$ are the shear force exerted by middle phase and pinning force caused by surface tension, respectively.

d_1 can be predicted by solving Eqs. (1), (6), and (7)[26] and d_2 can be predicted by mass balance assumption $d_2 = [(Q_1+Q_2)/Q_1)]^{\frac{1}{3}}d_1$.[24]

In our W/O/W double emulsion system, the middle jet breaks up first at the orifice of the collection capillary to form monodisperse droplets, as shown in Figure 2(A). We test the validity of Eqs. (4) and (5) by comparing the droplet sizes observed experimentally. The surface tension value for the bare interfaces between the middle-outer phases is $\gamma_{2,3} = 25.2$ mN/m. The tip diameters of our injection and collection capillary are 18 μm and 88 μm, respectively. An increase in Q_1 leads to increases of d_1 and d_2 while keeping other flow rates constant; whereas an increase in Q_2 results in a decrease in d_1 and an increase in d_2. The predicted values are in agreement with the experimental values acquired by image analysis, as shown in Figures 2(B) and 2(C). However, in our O/W/O emulsion systems, where the viscosity of middle phase is 27.5 times higher than that of the outer phase, the inner phase breaks up first and triggers the middle phase to pinch off, as shown in Figure 2(D). In this case, Eqs. (4) and

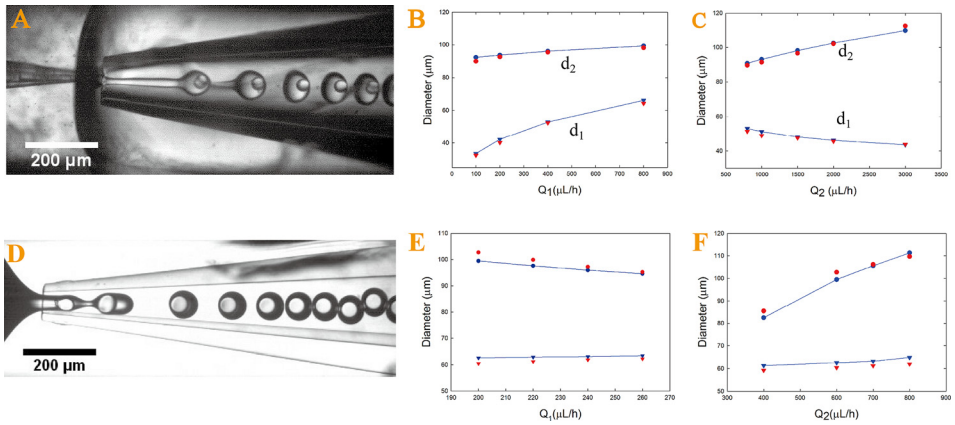

FIG. 2. Optical microscopic images of (A) microfluidic generation of W/O/W double emulsions; inner droplet size d_1 and the whole droplet size d_2 are predicted using Eqs. (4) and (5) (blue symbols) and compared with size measured through image analysis (red symbols) for changing Q_1 (B) and Q_2 (C) while keeping other flow rates constant. Optical microscopic images of (D) microfluidic generation of monodisperse O/W/O double emulsion droplets in a modified geometry; inner droplet size d_1 and the whole droplet size d_2 are predicted using Eqs. (6) and (7) (blue symbols) and compared with sizes measured by image analysis (red symbols) for changing Q_1 (E) and Q_2 (F) while keeping other flow rates as constant.

(5) fail to predict the size of the generated double emulsion droplets. Increase in Q_1 will speed up the growth of the inner droplet in size and expedite its detachment from the capillary tip. As the inner fluid quickly moves into the collection capillary, this causes the middle fluid to break up before its critical capillary number is reached, leading to a decrease in d_2 and thinner shells. However, Eq. (5) suggests that d_2 increases with increasing Q_1 and clearly contradicts the experimental observation. To address this, we predict d_1 and d_2 by solving Eqs. (6) and (7). The surface tension for the interface between inner and middle phase is 14 mN/m. The diameters of injection capillary and collection capillary are 25 μm and 80 μm, respectively. The derivation of Eqs. (6) and (7) indicates that d_1 increases with an increasing Q_1 and a decreasing Q_2 while d_2 increases with a decreasing Q_1 and an increasing of Q_2. The experimental data by image analysis agrees reasonably well with the prediction by Eqs. (6) and (7), as shown in Figures 2(E) and 2(F).

Due to the high degree of control offered by microfluidics, the size of emulsion droplets can also be tuned by varying the osmotic pressure difference between the inner and outer aqueous phases.[25] Due to the presence of a concentration gradient, when the osmolality of the inner phase is lower than that of outer phase, the solvent in the inner droplets start to diffuse out and causes the inner droplets to shrink, as shown in Figure 3(A). Before droplets are solidified, a large osmolality difference leads to a significant reduction in the inner and whole droplet size, as shown in Figure 3(B).

After the formation of W/O/W and O/W/O emulsion droplets, the droplets are solidified into monodisperse core-shell alginate-PLGA and PLGA-alginate microspheres, respectively. For W/O/W emulsion droplets, calcium ions in the outer phase diffuse through the oil layer and crosslink the alginate in the inner droplets to form calcium alginate microspheres, as shown in Figures 4(A) and 4(B). PLGA in the oil layer solidifies to form a shell that surrounds alginate microspheres after the complete evaporation of DCM. The resultant core-shell particles are shown in Figure 4(C). Silver nanoparticles and a hydrophobic dye, Oil Red O, are added to the inner and middle phases, respectively, as model hydrophilic and hydrophobic active ingredients. They are encapsulated in the cores and the shells of the resultant microspheres as shown in Figure 4(D). The O/W/O emulsion droplets are collected in a mixture of ethanol and calcium chloride with a volume ratio of 1:3. The calcium ions in the collection mixture diffuses into the droplet shells and crosslink the sodium alginate, resulting in solidified PLGA microspheres surrounded by calcium alginate shells, as illustrated in Figure 4(E). Due to its miscibility with both water and toluene, ethanol is added to speed up the diffusion of calcium ions. The resultant core-shell microspheres are shown in Figures 4(F) and 4(G); the alginate shell is stained

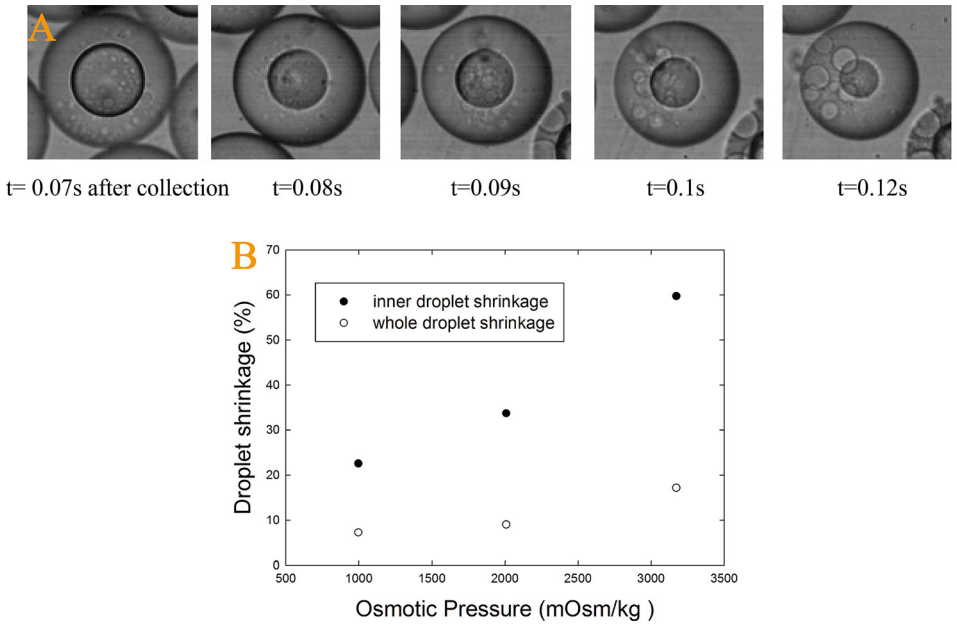

FIG. 3. (A) Optical microscopic image demonstrating droplet size change over time due to a difference in osmolality between the inner and the continuous phases; (B) A plot of the droplet size reduction as a function of differences in osmolality before solidification.

with alcian blue for visualization, as shown in Figure 4(G). The core-shell structure is confirmed by variable-pressure SEM with core size and overall particle size are 53.2 μm and 68.5 μm, respectively, as shown in Figure 4(H).

With alginate-PLGA and PLGA-alginate core-shell microspheres, the functionality as well as versatility as a potential drug carrier is improved, when compared to single microspheres. For alginate-PLGA microspheres, the alginate cores have a high loading efficiency for hydrophilic actives, while PLGA shells can prevent undesired leakage and release these encapsulated actives in a sustained manner. For PLGA-alginate microspheres, the alginate shells can modulate release kinetics of hydrophobic actives from PLGA cores. Typical high initial drug release

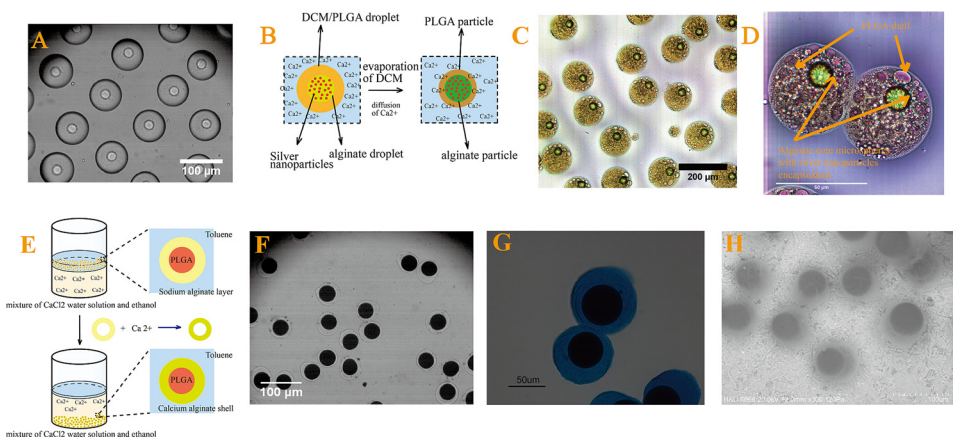

FIG. 4. Optical microscopic image of (A) collection of W/O/W double emulsion droplets, (B) schematic illustrating the solidification of an emulsion droplet into alginate-PLGA core-shell microspheres, (C) and (D) optical microscope images of alginate-PLGA core-shell microspheres with silver nanoparticles and dye Oil Red O encapsulated in the core and shell, respectively, (E) schematic illustration of the collection of emulsion droplets that subsequently solidifies due to crosslinking by the calcium ions, (F) and (G) optical microscopic image, and (H) variable-pressure SEM image of PLGA-alginate core-shell microspheres. The alginate shells are stained for visualization in (G).

rate from PLGA microspheres is largely due to rapid release of drugs from the surface. With alginate shells, drugs on the surface of PLGA cores must first diffuse through the alginate matrices before release; as a result, the initial release rate is reduced and the release period is prolonged.[26] This is favorable in most sustained release applications since a high initial release rate usually leads to a loss of active ingredients and thus a shortened release period.

Release profile from core-shell microspheres can be designed by tailoring shell properties such as the mesh size of matrices and shell thickness to achieve profiles difficult to achieve with single microspheres. The monodispersity of core-shell microspheres enables the investigation of the relationship between the release kinetics and microstructures. This potentially enables pre-determined release profile of actives.

Our core-shell microspheres can encapsulate and release active ingredients of different properties in a sustained manner. By choosing a combination of materials with different release mechanisms, a diverse range of release profile can be tailor-designed based on the needs of applications. This makes them suitable for delivery of drugs, proteins and genes for biomedical research and applications.

CONCLUSIONS

Polymer-based systems are promising delivery vehicles for biomedical applications. Core-shell structured polymeric microspheres demonstrate multiple functionalities, when comparing with conventional single microspheres. Core-shell polymer microspheres fabricated by microfluidics are monodisperse, with precisely and easily tuned core size and shell thickness. Release kinetics is significantly influenced by incorporating a shell layer. By inserting an alginate core to PLGA microspheres, the encapsulation efficiency is enhanced and delicate hydrophilic active ingredients such as DNA and siRNA are protected from organic solvent by the hydrogel core. Similarly, an alginate shell can also be added to PLGA cores; this reduces the initial release of the active ingredient, thus extending the overall release period. The effect of shell properties, such as shell thickness and porosity, can be manipulated to modulate the release profile from core-shell particles. The approach of using core-shell particles as delivery vehicles also enables co-delivery of active ingredients with different solubility by encapsulating them separately in the core and the shell. Monodisperse polymer-based core-shell microspheres provide a platform for systematic studies of controlled release. Furthermore, the monodispersity and reproducibility of these microspheres suggest new opportunities to investigate the relationship between characteristics of microspheres and their release kinetics. This will provide the information needed for tailoring the release profile to the need of the application. Moreover, additional functional groups and reagents can be incorporated into the shell to realize targeted delivery and on-demand release. Therefore, core-shell particles represent a first step towards delivery vehicle that can deliver and release the needed amount of active ingredients to the target location with high efficiency upon specific triggers.

ACKNOWLEDGMENTS

We gratefully acknowledge financial support from the Seed Funding Programme from the University of Hong Kong (201101159009, 201109160030, and 201109176165), the Science and Technology Innovation Commission of Shenzhen Municipality (JC201105190878A), National Natural Science Foundation of China (NSFC51206138/E0605) and the Research Grants Council of Hong Kong (GRF718009, GRF718111, GRF717613, and HKU707712P). This research is also supported in part by the Zhejiang Provincial, Hangzhou Municipal and Linan County Governments.

[1]D. Scheffert and E. Wagner, Gene Ther. **15**, 1131 (2008).
[2]D. W. Pack, A. S. Hoffman, S. Z. Pun, and P. S. Stayton, Nat. Rev. Drug Discovery **4**, 581 (2005).
[3]V. R. Sinha and A. Trehan, J. Controlled Release **90**, 261 (2003).
[4]S. Freiberg and X. X. Zhu, Int. J. Pharm. **282**, 1 (2004).
[5]H. Okada and H. Toguchi, Crit. Rev. Ther. Drug Carrier Syst. **12**, 1 (1995).
[6]J. M. Anderson and M. S. Shive, Adv. Drug Delivery Rev. **28**, 5 (1997).
[7]S. Cohen, T. Yoshioka, M. Lucarelli, L. H. Hwang, and R. Langer, Pharm. Res. **8**, 713 (1991).

[8]Y. Y. Yang, T. S. Chung, and N. P. Ng, Biomaterials **22**, 231 (2001).
[9]X. Huang and C. S. Brazel, J. Controlled Release **73**, 121 (2001).
[10]U. Edlund and A.-C. Albertsson, Adv. Polym. Sci. **157**, 67 (2002).
[11]N. Nihant, C. Schugens, C. Grandfils, R. Jerome, and P. Teyssie, J. Colloid Interface Sci. **173**, 55 (1995).
[12]Y. Yeo and K. Park, Arch. Pharmacal Res. **27**, 1 (2004).
[13]R. K. Shah, H. C. Shum, A. C. Rowat, D. Lee, J. J. Agresti, A. S. Utada, L. Y. Chu, J. W. Kim, A. Fernandez-Nieves, C. J. Martinez, and D. A. Weitz, Mater. Today **11**, 18 (2008).
[14]H. C. Shum, J. W. Kim, and D. A. Weitz, J. Am. Chem. Soc. **130**, 9543 (2008).
[15]H. C. Shum, D. Lee, I. Yoon, T. Kodger, and D. A. Weitz, Langmuir **24**, 7651 (2008).
[16]S. W. Choi, Y. Zhang, and Y. Xia, Adv. Funct. Mater. **19**, 2943 (2009).
[17]J. W. Kim, A. S. Utada, A. Fernandez-Nieves, Z. Hu, and D. A. Weitz, Angew. Chem. **119**, 1851 (2007).
[18]A. S. Utada, E. Lorenceau, D. R. Link, P. D. Kaplan, H. A. Stone, and D. A. Weitz, Science **308**, 537 (2005).
[19]W. R. Gombotz and S. F. Wee, Adv. Drug Delivery Rev. **31**, 267 (1998).
[20]C. C. Ribeiro, C. C. Barrias, and M. A. Barbosa, Biomaterials **25**, 4363 (2004).
[21]M. George and T. E. Abraham, J. Controlled Release **114**, 1 (2006).
[22]M. Lian, C. P. Collier, M. J. Doktycz, and S. T. Retterer, Biomicrofluidics **6**, 044108 (2012).
[23]R. M. Erb, D. Obrist, P. W. Chen, J. Studer, and A. R. Studart, Soft Matter **7**, 8757 (2011).
[24]See supplementary material at http://dx.doi.org/10.1063/1.4819274 for the deduction of the model to predict sizes of the double emulsion droplets in a flow-focusing geometry assuming the break-up of the inner or middle phase triggers the formation of double emulsion droplets.
[25]F. Q. Tu and D. Lee, Langmuir **28**, 9944 (2012).
[26]J. Wu, T. Kong, K. W. K. Yeung, H. C. Shum, K. M. C. Cheung, L. Wang, and M. K. T. To, Acta Biomater. **9**, 7410 (2013).